Promoting Effect of CeO_2 in Combustion Synthesized Pt/CeO_2 Catalyst for CO Oxidation

Parthasarathi Bera,[†] Arup Gayen,[†] M. S. Hegde,*[,†] N. P. Lalla,[‡] Lorenzo Spadaro,[§] Francesco Frusteri,[§] and Francesco Arena[§]

Solid State and Structural Chemistry Unit, Indian Institute of Science, Bangalore-560012, India, Inter University Consortium for DAE Facilities, University Campus, Indore-452017, India, and Istituto CNR-TAE, Salita S. Lucia 39, I-98126 S. Lucia, Messina, Italy

Received: September 24, 2002

A 1% Pt/CeO_2 catalyst prepared by the solution combustion method shows a higher catalytic activity for CO oxidation by O_2 compared to Pt metal particles. At least six hydrogen atoms are taken up per Pt at −25 °C. The structure of 1% Pt/CeO_2 catalyst has been investigated by X-ray diffraction (XRD), transmission electron microscopy (TEM), X-ray photoelectron spectroscopy (XPS), and Fourier transform infrared (FTIR) spectroscopy. Rietveld refinement shows that Pt ions are incorporated into the CeO_2 matrix in the form of $Ce_{1-x}Pt_xO_{2-\delta}$ solid solution. A decrease in oxygen content in 1% Pt/CeO_2 is seen in relation to pure CeO_2. TEM studies show that Pt is dispersed as atoms or ions and only a small amount as Pt metal particles. The Pt(4f) core level region in XPS shows that Pt is present mostly in the Pt^{2+} ionic state on CeO_2 surface. FTIR of 1% Pt/CeO_2 shows a strongly adsorbed CO peak at 2082 cm^{-1} corresponding to oxidized Pt. These structural studies show that Pt ions in the catalyst are substituted for Ce^{4+} ions in the form of $Ce_{1-x}Pt_xO_{2-\delta}$, creating oxide ion vacancies leading to a strong $Pt^{2+}-CeO_2$ interaction that is responsible for higher catalytic activity.

Introduction

The catalytic activity of dispersed metals on a support is influenced by a number of factors, namely, size, shape, extent of dispersion, relative amount of metals present, chemical nature of the support, and the strength of interaction between the support and the metal.[1] Supported and unsupported Pt are promising catalysts in the control of pollutant gas emission.[2−10] It is observed that interaction between noble metal such as Pt with ceria enhances the catalytic activities.[11−18] The promoting action of CeO_2 is attributed to oxygen storage capacity (OSC), higher reducibility in the presence of Pt, higher dispersion of Pt over CeO_2 compared to Al_2O_3, and prevention of sintering of Pt metal particles. Carbon monoxide and hydrocarbon oxidation and NO reduction are the typical auto exhaust catalytic reactions, and addition of CeO_2 has shown higher rates of conversion at lower temperatures compared to the same Pt dispersed over Al_2O_3.[16] Summers and Ausen[12] have suggested that CeO_2 promotes oxidation of Pt. Therefore, an insight into the exact chemical interaction between Pt and CeO_2 in enhancing the catalytic activities of Pt/CeO_2 compared to pure Pt metal can be deduced from the electronic and atomic structure of Pt/CeO_2 catalyst. Hoflund et al.[19−23] and Haruta et al.[24−26] have observed a similar promoting effect toward low-temperature CO oxidation over noble metals/reducible oxide support catalysts such as Pt/SnO_x, Au/MnO_x, Pt/TiO_2, Au/Fe_2O_3, and Au/Co_3O_4. Pt is shown to be bonded through surface lattice oxygen, giving Sn−O−Pt surface species in Pt/SnO_x.[19] This bonded Pt is not completely reducible even at high-temperature reduction, indicating a strong chemical interaction between Pt and SnO_x.

Recently, we have synthesized ceria and alumina supported metal catalysts by the solution combustion method and studied their catalytic activities.[27−29] To understand the promoting effect of CeO_2, we have investigated the structure of Pt/CeO_2 catalyst by XRD, TEM, XPS, and FTIR techniques and carried out comparative catalytic studies on Pt/CeO_2 prepared by the combustion method with fine Pt metal particles. Here, we show that platinum ions present in the form of a $Ce_{1-x}Pt_xO_{2-\delta}$ solid solution in the combustion synthesized Pt/CeO_2 catalyst are the active sites, and the promoting action of CeO_2 is attributed to the accessibility of the Ce^{4+}/Ce^{3+} redox couple with Pt^{2+}/Pt^0 through oxide ion vacancies.

Experimental Section

Synthesis. The combustion mixture for the preparation of 1% Pt/CeO_2 contained $(NH_4)_2Ce(NO_3)_6$, H_2PtCl_6, and $C_2H_6N_4O_2$ (oxalyldihydrazide) in the mole ratio 0.99:0.01:2.38. Oxalyldihydrazide (ODH) prepared from diethyl oxalate and hydrazine hydrate was used as the fuel. In a typical preparation, 10 g of $(NH_4)_2Ce(NO_3)_6$ (E. Merck India Ltd., 99.9%), 0.095 g of H_2PtCl_6 (Ranbaxy Laboratories Ltd., 99%), and 5.175 g of ODH were dissolved in the minimum volume of water (30 cm^3) in a borosilicate dish of 300 cm^3 capacity. The dish containing the redox mixture was introduced into a muffle furnace maintained at 350 °C. Initially the solution boiled with frothing and foaming and underwent dehydration. At the point of complete dehydration, the surface ignited, burning with a flame (∼1000 °C) and yielding a voluminous solid product within 5 min. Similarly, 0.1 to 0.5, 2% Pt/CeO_2 catalysts were prepared by this method. These compounds were prepared in an open muffle furnace kept in a fume cupboard with exhaust. The reaction could be controlled by carrying out the combustion in an open vessel. As-prepared combustion products without further treatment such as reduction by H_2 or any heat treatment are used for all the studies including the catalytic reactions. Fine Pt particles were prepared by the polyol method. H_2PtCl_6 was

* Corresponding author. E-mail: mshegde@sscu.iisc.ernet.in; partho@sscu.iisc.ernet.in; Fax: +91-80-3601310.
[†] Indian Institute of Science.
[‡] Inter University Consortium for DAE Facilities.
[§] Istituto CNR-TAE.

10.1021/jp022132f CCC: $25.00
Published on Web 05/28/2003

reduced in ethylene glycol solution at 180 °C, giving Pt particles of 6−7 nm as seen from TEM studies.

Temperature Programmed Reaction (TPR). The catalytic reactions were carried out in a temperature programmed reaction system equipped with a quadrupole mass spectrometer QXK300 (VG Scientific Ltd., England) for product analysis in a packed bed tubular reactor at atmospheric pressure. Typically, 100 mg of Pt/CeO_2 catalyst (40/80 mesh) diluted with 100 mg of SiO_2 (30/60 mesh) was loaded in a quartz tube reactor of 250 mm length and 4 mm internal diameter and endings were plugged with ceramic wool. The reactions were also carried out over fine Pt powder mixed with SiO_2, where the quantity of polyol prepared Pt powder taken was 2.2 times the amount of Pt present in 100 mg of 1% Pt/CeO_2 catalyst. The sample temperature was measured by a fine chromel−alumel thermocouple immersed in the catalyst bed. The gas flow was controlled using mass flow sensors (Honeywell AWM3100V and Bronkhorst Hi-Tech BV) calibrated against a standard bubble flow meter. The inlet gas composition was CO (4.35 vol %), O_2 (13 vol %) with He as balance, keeping total flow at 69 sccm to achieve gas hourly space velocity (GHSV) of 30 000 h^{-1} unless otherwise mentioned. The reactions were carried out as a function of temperature with a linear heating rate of 5° min^{-1}. Reactions were also performed in step temperature mode (5 min at each temperature) from 50 to 300 °C in steps of 5° to compare the characteristics of CO + O_2 reaction with linear heating mode. CO oxidation over 1% Pt/CeO_2 was also carried out at 220 °C for 25 h with the same 30 000 h^{-1} GHSV to obtain the decay characteristics. The gaseous products were sampled through a fine control leak valve to an ultrahigh vacuum (UHV) system housing the quadrupole mass spectrometer at 10^{-9} Torr. Final pressure of the gases in the vacuum system was 2×10^{-5} Torr. All the masses were scanned in every 10 s. At the end of the reaction, the intensity of each mass as a function of temperature (thermogram) was generated. The gas mixture (5% CO in He) and oxygen were obtained from Bhoruka Gases Ltd., Bangalore. The purity of the gas mixture and O_2 was 99.9%.

H_2 Uptake Measurement. Hydrogen uptake experiments were carried out in a continuous flow gradientless microreactor of length 200 mm and 4 mm diameter with 6% H_2/Ar flowing at 30 STP cm^3 min^{-1}. Hydrogen concentration was monitored by a thermal conducting detector (TCD) connected to a personal computer for data storage. The TCD response was quantitatively calibrated by monitoring the reduction of a known amount of CuO.

Characterization. XRD data of the materials for Rietveld refinement were collected on a Rigaku-2000 diffractometer with a rotating anode using CuKα radiation having a graphite-crystal monochromator. Data were obtained at a scan rate of 1° min^{-1} with 0.02° step size in the 2θ range 10 to 110°, and the structure was refined using the FullProf-98 program. The number of parameters refined simultaneously was 19.

A JEOL JEM-200CX transmission electron microscope operated at 200 kV was used to carry out TEM studies.

The BET surface area was measured by low-temperature N_2 adsorption employing a Micromeritics Accusorb 2100 E surface area analyzer.

XPS of as-prepared catalysts were recorded in an ESCA-3 Mark II spectrometer (VG Scientific Ltd., England) using AlKα radiation (1486.6 eV). Binding energies were calculated with respect to C(1s) at 285 eV. Binding energies were measured with a precision of ± 0.2 eV. XPS of 1% Pt/CeO_2 catalyst after CO + O_2 reaction at 220 °C for 25 h was also carried out. For XPS analysis, the powder samples were made into pellets of 8 mm diameter employing 12 kN pressure and placed into an ultrahigh vacuum (UHV) chamber at 10^{-9} Torr housing the analyzer. The experimental data were curve fitted with Gaussian peaks after subtracting a linear background.

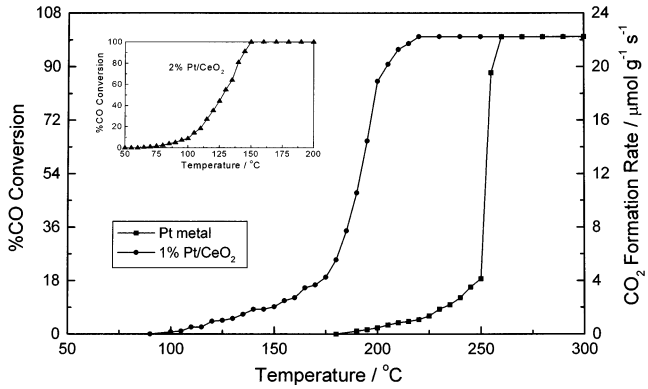

Figure 1. %CO conversion and corresponding rates for CO + O_2 reaction on (a) 1% Pt/CeO_2 and (b) Pt metal particles at 30 000 h^{-1} GHSV. (Inset: %CO conversion for CO + O_2 reaction on 2% Pt/CeO_2 at 11 000 h^{-1} GHSV).

FTIR spectra of CO over Pt nanoparticles and Pt/CeO_2 catalyst were recorded on a Perkin-Elmer Spectrum 2000 FTIR spectrometer equipped with a DRIFT unit (Graseby Specac, UK) in the 750−4000 cm^{-1} wavenumber region with a resolution of 4 cm^{-1}. The sample (50 mg) was placed in a stainless steel IR cell containing zinc selenide windows. The cell is connected to a conventional vacuum/gas handling system. For the experiments run under flowing conditions at atmospheric pressure, a gas flow of 30 cm^3 min^{-1} was used with the gas composition of 5% CO in He at room temperature. The sample could be heated to 500 °C.

Results

TPR Studies. CO oxidation by O_2 was carried out over 1% Pt/CeO_2 and polyol synthesized Pt fine metal particles at a gas hourly space velocity (GHSV) of 30 000 h^{-1}. The rate of CO_2 formation along with percentage CO conversion over these catalysts as a function of temperature are presented in Figure 1. The light-off temperature (temperature at 50% conversion) is 190 °C for 1% Pt/CeO_2, whereas the light-off temperature is observed at 255 °C for fine Pt metal particles. It must be noted that 1.13 mg of Pt is present in 100 mg of 1% Pt/CeO_2 catalyst, and 2.5 mg of Pt particles (6−7 nm) diluted with SiO_2 was taken in our experiment. Percent conversions and corresponding rates are the same whether the reaction was carried out at a heating rate of 5° min^{-1} or in the step temperature mode of 5 min at each temperature from 50 to 300 °C. The light-off temperature of the CO + O_2 reaction over $Pt/CeO_2/Al_2O_3$ and Pt/Al_2O_3 reported by Martínez-Arias et al.[16] compares well with our study on Pt/CeO_2 and Pt metal particles. They have taken 300 mg of the catalyst (0.5 wt % Pt) at the same GHSV of 30 000 h^{-1} with 1% CO. With 4.35 vol % CO taken in our experiment, rate of conversion is therefore 4 to 5 times higher in our present study than what is obtained by Martínez-Arias et al. over $Pt/CeO_2/Al_2O_3$. CO oxidation over 2% Pt/CeO_2 was also performed at a lower GHSV of 11 000 h^{-1} with the same 4.35 vol % CO. Light-off temperature is 130 °C (see inset of Figure 1). The activation energy (E_a) has also been calculated from Arrhenius plots of ln(rate) vs $1/T$ for the CO + O_2 reaction. Here, CO_2 formation rates were taken into account to calculate the activation energy. Activation energy for the CO + O_2 reaction over 1% Pt/CeO_2 is 44 kJ mol^{-1}, whereas it is 88 kJ

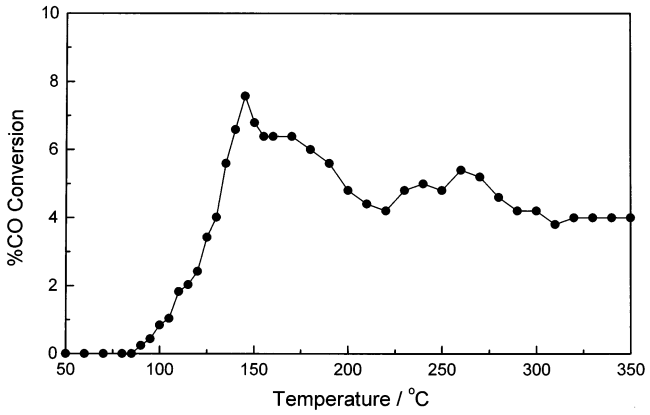

Figure 2. %CO conversion for TPR of CO on 1% Pt/CeO_2 as a function of temperature.

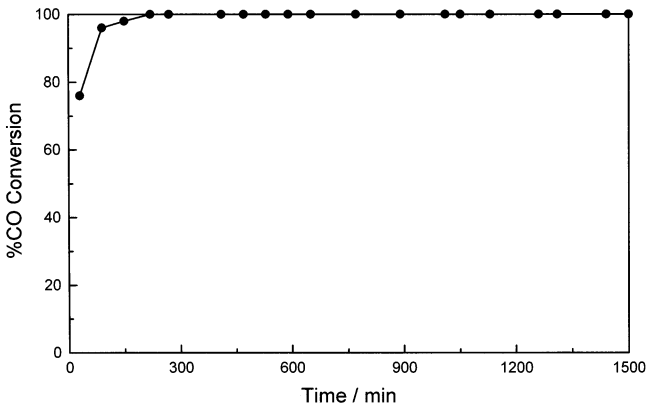

Figure 3. CO oxidation activity of 1% Pt/CeO_2 at 220 °C as a function of time.

mol^{-1} over Pt metal particles. Therefore, a large decrease in the CO oxidation temperature, higher rates of conversion at lower temperatures, and low activation energy over Pt/CeO_2 observed are due to the promoting effect of CeO_2.

To examine whether lattice oxygen is utilized for CO_2 formation during CO oxidation, TPR was carried out over 2% Pt/CeO_2 flowing only CO + He with 1.5 vol % CO per min at the same 30 000 h^{-1} GHSV. In Figure 2, %CO conversion to CO_2 as a function of temperature is given. Clearly, it is observed that lattice oxygen is utilized during CO_2 formation at a temperature similar to that with feed oxygen (compare Figure 2 with inset of Figure 1). However, the percent CO conversion is low. With feed oxygen, the percent CO conversion is higher indicating that molecular (feed) oxygen is dissociated on the catalyst surface.

The catalytic activity of the CO + O_2 reaction over 1% Pt/CeO_2 as a function of time at 220 °C is also investigated and it is shown in Figure 3. The GHSV for this constant temperature reaction was 30 000 h^{-1}. An increase in the percent conversion is seen initially, and after 150 min the reaction approaches a steady state complete conversion. Thereafter, no deactivation of the catalyst is observed even up to 25 h on stream reaction. In a recent study, combustion synthesized 2% Pt/CeO_2 was employed for partial oxidation of CH_4 and the catalyst did not show deactivation even up to 100 h.[30]

H_2 Uptake Studies. H_2 uptake experiment was carried out over 0.1 to 2% Pt/CeO_2 prepared by the solution combustion method from −80 to 720 °C. Figure 4 shows temperature programmed reduction profiles for 1 and 2% Pt/CeO_2, pure CeO_2, and $H_2Pt(OH)_6$. Pure CeO_2 shows H_2 uptake (oxygen storage capacity) from 200 to 480 °C, and the total volume of

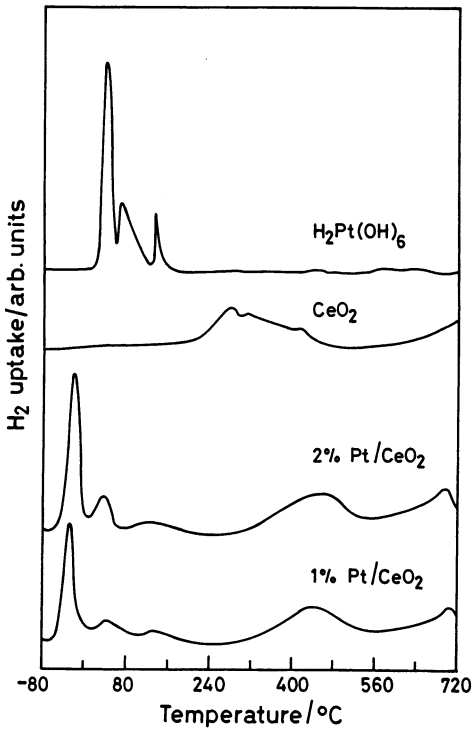

Figure 4. H_2 uptake over $H_2Pt(OH)_6$, CeO_2, 2% Pt/CeO_2, and 1% Pt/CeO_2 as a function of temperature.

hydrogen is 28 $cm^3\ g^{-1}$ of CeO_2, which is equivalent to 14 cm^3 of $O_2\ g^{-1}$. This corresponds to the reduction of CeO_2 to $CeO_{1.89}$. Temperature for H_2 uptake as well as the extent of CeO_2 reduction is indeed comparable to the results reported in the literature.[31,32] H_2 uptake over Pt/CeO_2 samples occurs between −40 and 80 °C with a main peak at −25 °C over 1% Pt/CeO_2 in addition to a CeO_2 related peak at 450 °C. The H_2 uptake peak is observed at 40 °C over $H_2Pt(OH)_6$ and the volume of hydrogen adsorbed corresponds to the reaction $Pt^{4+} + 2H_2 \rightarrow (Pt^0 - 4H^+)$. The low-temperature H_2 uptake peak at −25 °C is thus related to platinum species present in Pt/CeO_2. Smaller peaks at the 40−120 °C region may be due to Pt^{4+} reduction, which is in the same range of Pt^{4+} reduction in $H_2Pt(OH)_6$. The total amount of hydrogen due to Pt over Pt/CeO_2 at temperatures below 80 °C is estimated, and in Figure 5 the mole ratios of hydrogen to Pt as a function of % Pt loading are shown. As the Pt concentration on CeO_2 increases, the H_2/Pt mole ratio decreases. Three moles of hydrogen are taken up in the 1% Pt/CeO_2 sample at low temperature. Reaction of adsorbed H_2 over Pt/CeO_2 with O_2 at room temperature was also performed. After the H_2 adsorption over 1% Pt/CeO_2 up to 100 °C, the sample was cooled to 25 °C in H_2/Ar flow. The sample was purged with pure Ar and then O_2 was admitted to the sample in pulsed mode at 25 °C. The amount of oxygen utilized was exactly half of the total volume of hydrogen adsorbed, indicating that at 25 °C, H_2 is utilized to form H_2O. Hydrogen was readsorbed over the same catalyst and the amount of hydrogen uptake was the same as in Figure 4.

The hydrogen uptake experiment and its subsequent reaction with oxygen shows that 3 mol of hydrogen is adsorbed over 1% Pt/CeO_2 at temperature much lower than pure Pt or Pt/Al_2O_3 reported in the literature.[33,34] Over pure Pt, the number of hydrogen atoms adsorbed is at best one atom per surface Pt atom. Over Pt/Al_2O_3, adsorption of 2−3 hydrogen atoms per Pt atom is seen at relatively higher temperature (200 °C) and it is described as due to hydrogen spillover.[33,34] The Pt/CeO_2 system certainly is different in two ways. First, the number of

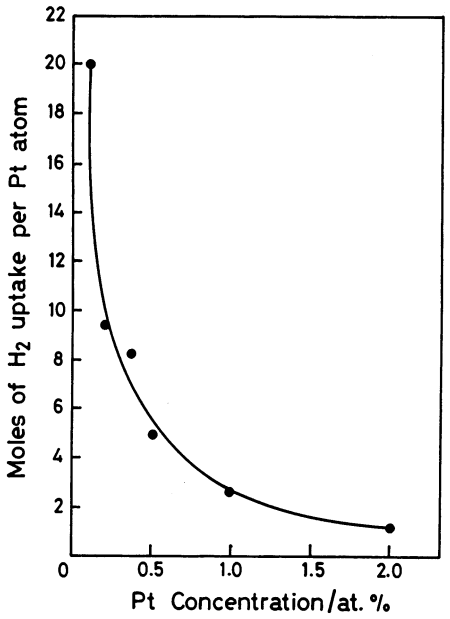

Figure 5. Moles of H_2 uptake per Pt atom as a function of Pt concentration.

hydrogen atoms taken up per Pt is 6 in 1% Pt/CeO_2, which is much higher than on pure Pt or Pt/Al_2O_3, and, second, it occurs at a much lower temperature. A similar observation has been made recently by Hickey et al.[35] Higher amount of hydrogen uptake at low temperature can be attributed to hydrogen spillover phenomena over Pt/CeO_2. The $H_2 + O_2$ reaction at room temperature suggests that hydrogen is in dissociated form. High rates of $2H_2 + O_2 \rightarrow 2H_2O$ have been observed at 25 °C in our earlier studies.[36,37] Therefore, a much larger amount of H_2 uptake at lower temperature over Pt/CeO_2 than Pt/Al_2O_3 is attributed to the promoting effect of CeO_2.

XRD Studies. A careful XRD study was undertaken to see whether platinum ions are incorporated into the CeO_2 matrix in 1% Pt/CeO_2 catalyst. Observed, calculated, and difference XRD patterns of 1% Pt/CeO_2 are shown in Figure 6. Rietveld refinements are carried out by varying 19 parameters such as overall scale factor, background parameters, unit cell, shape, and isotropic thermal parameters along with oxygen occupancy. The diffraction lines are indexed to fluorite structure ($Fm3m$). In 1% Pt/CeO_2, the R_{Bragg}, R_F, and R_P values are 1.31, 0.819, and 3.4% respectively. The lattice parameter a is 5.41048 ± 0.00012 Å. Pure CeO_2 was also refined, and R_{Bragg}, R_F, and R_P are 0.914, 0.689, and 4.45% respectively. The a value for pure CeO_2 is 5.41128 ± 0.00025 Å. Total oxygen in 1% Pt/CeO_2 is 1.883 and that in pure CeO_2 is 1.934. The quality of X-ray data is to be considered good from excellent signal to noise ratio. In 1% Pt/CeO_2, no impurity lines are seen corresponding to any of the platinum oxides. Even though the X-ray scattering factor of oxygen is low compared to cerium, the absolute oxygen content obtained from the refinement can give us trends in the variation of oxygen content. A decrease of oxygen content from 1.934 in pure CeO_2 to 1.883 in 1% Pt/CeO_2 is significant. Decrease in the lattice parameter in 1% Pt/CeO_2 compared to pure CeO_2 is statistically significant. In Figure 6, a small broad hump at $2\theta = 39.8°$ due to Pt (111) can be seen in the pattern when the region is expanded in the y-axis, indicating the presence of trace amounts of Pt metal particles. To examine the expected Pt (111) peak intensity in the XRD pattern, polyol synthesized Pt particles (6−7 nm) were physically mixed with pure CeO_2 to 1 at. % Pt level and XRD was recorded. The 1% Pt/CeO_2 catalyst and 1% Pt + CeO_2 XRD patterns are blown up to the same scale with reference to the CeO_2 (111) peak. The intensity ratio of Pt (111) in 1% Pt/CeO_2 to that in 1% Pt + CeO_2 physical mixture is 0.08. Thus, XRD studies show that at least 0.92 at. % of the platinum taken in the preparation of 1 at. % Pt/CeO_2 is incorporated in the CeO_2 lattice. Therefore, Rietveld analysis does indicate the possible substitution of platinum ions in Ce^{4+} sites in the CeO_2 matrix. Similarly, Rietveld analysis of 2% Pt/CeO_2 shows over 0.18% Pt metal on CeO_2. Peaks due to PtO or PtO_2 could not be detected in both the catalysts even to the extent of Pt metal.

TEM Studies. Typical TEM images of as-prepared 1% and 2% Pt/CeO_2 are given in Figure 7. Average sizes of CeO_2 crystallites are in the range of 30 ± 7 nm. The morphology of CeO_2 crystallites is cubic. Very few Pt particles can be seen on CeO_2 crystallites in 1% Pt/CeO_2 catalyst (Figure 7a). The number of Pt particles are higher in case of 2% Pt/CeO_2 (Figure 7b). In contrast, nanosized fine Pt metal particles can be dispersed on α-Al_2O_3 by the solution combustion method[28] and the number of Pt particles is much higher for the same amount of Pt taken in the preparation (Figure 7c). The average sizes of Pt particles on α-Al_2O_3 are 7−10 nm, whereas Pt particles detectable in 1% Pt/CeO_2 are smaller in size (4−5 nm). The polycrystalline electron diffraction pattern of 1% Pt/CeO_2 could be indexed to CeO_2 with fluorite structure. Thus, TEM studies demonstrate that over as-prepared 1% Pt/CeO_2 an extremely small amount of Pt is present as metal particles and the rest is apparently dispersed as atoms or ions that could not be detected.

The BET surface area of as-prepared 1% Pt/CeO_2 is 26 $m^2\ g^{-1}$. The average size of Pt/CeO_2 as seen from TEM is 30 nm. Considering that Pt/CeO_2 consists of 30 nm cubic crystallites, total surface area per gram of Pt/CeO_2 particles comes out to be 27.7 $m^2\ g^{-1}$, which is close to the experimentally observed value. This indicates that Pt/CeO_2 prepared by the solution combustion method are nanocrystallites and that there is no contribution from amorphous CeO_2 to the surface area. This conclusion is supported by the flat background of the XRD pattern in Figure 6.

XPS Studies. XPS survey spectra obtained from 1% Pt/CeO_2 catalyst sample before and after CO + O_2 reaction are shown in Figure 8. They exhibit predominant core level peaks due to Ce, O, C, and Pt. There is no peak corresponding to Cl.

Ce(3d) peaks obtained from 1% Pt/CeO_2 sample before and after the reaction are given in Figure 9. Ce($3d_{5/2,\ 3/2}$) peaks at 882.9 and 901.3 eV with characteristic satellites (marked in the figure) correspond to CeO_2 with Ce in the +4 oxidation state.[18,38] Intensity and positions of the Ce(3d) peaks remain the same after CO + O_2 reaction.

In Figure 10, C(1s) and O(1s) spectra in 1% Pt/CeO_2 before and after CO + O_2 reaction are shown. The C(1s) peak is observed at 285 eV and there is no significant change in the peak position in the spent catalyst. Further, the total intensity of C(1s) as well as the C(1s) to Ce(3d) integrated intensity ratio are also unchanged in the samples before and after the reaction. Similarly, the intense O(1s) peak at 530.3 eV in the as-prepared sample corresponds to CeO_2, which is unaltered after the reaction.

XPS of Pt(4f) core level region in Pt metal particles and 1% Pt/CeO_2 at different conditions are given in Figure 11. In Pt metal particles, $4f_{7/2,\ 5/2}$ peaks are observed at 71.1 and 74.3 eV, respectively, with full width at half maximum (fwhm) of 2.3 eV. XPS of as-prepared 1% Pt/CeO_2 could be resolved into three sets of spin−orbit doublets. Accordingly, Pt($4f_{7/2,\ 5/2}$) peaks at 71.0, 74.2; 71.9, 75.1; and 74.3, 77.5 eV could be assigned to Pt^0, Pt^{2+}, and Pt^{4+}, respectively, (Figure 11b).[18,39] Here, Pt

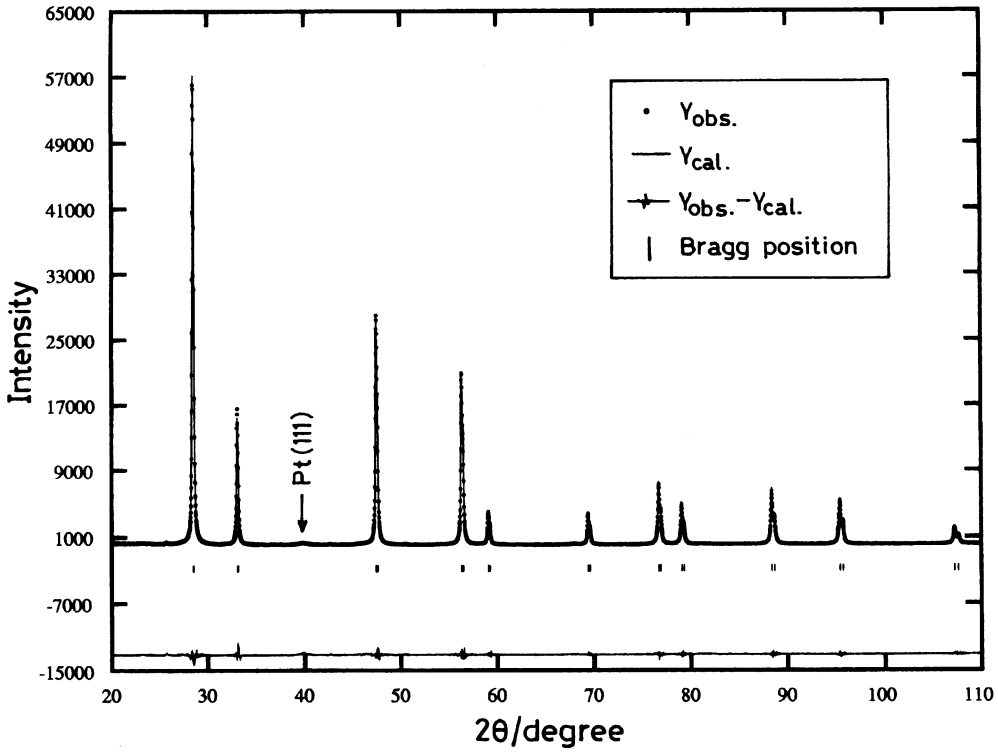

Figure 6. Observed, calculated, and difference XRD patterns of 1% Pt/CeO_2.

is found to be dispersed mostly in +2 (72%) and +4 (21%) oxidation states on CeO_2 crystallites with only about 7% Pt in the Pt^0 state. In the sample after the reaction for 25 h at 220 °C, Pt^{2+}(4f) peaks are shifted to higher binding energies by about 0.5 eV, whereas corresponding Pt^0 and Pt^{4+} peaks remain in the same positions. However, slight decrease in the fwhm of different Pt(4f) species is observed. To see if this binding energy shift is due to heating of the catalyst at 220 °C for a long period in excess O_2, a 1% Pt/CeO_2 sample was heated at 300 °C in air for 100 h and the XPS of this sample was recorded. There is no significant change in the O(1s) and Ce(3d) spectra. However, a shift in Pt^{2+}(4f) peaks to 0.4 eV higher binding energy compared to as-prepared Pt/CeO_2 is observed. Therefore, the shift in Pt^{2+}(4f) binding energy in the spent catalyst is due to the stabilization of Pt in the oxidized state in CeO_2 matrix in the course of CO + O_2 reaction under excess O_2. The XPS of Pt(4f) core level region of 2% Pt/CeO_2 given in Figure 11d also shows peaks corresponding to Pt^0 (12%), Pt^{2+} (69%) and Pt^{4+} (19%). Since Pt/CeO_2 reduced by H_2 takes up oxygen at room temperature, ex situ XPS of H_2-reduced Pt/CeO_2 is difficult. We have tried to reduce Pt/CeO_2 inside the preparation chamber of XPS at 1 atm pressure of H_2 at 200 °C for 1.5 h. Even though there are some changes in the XPS of Pt(4f) showing an increase in the intensity at lower binding energy region, Pt in Pt/CeO_2 could not be reduced to Pt metal as fully as in Pt metal particles. The reduced sample does also contain oxidized Pt species. On reoxidation with O_2 in the XPS chamber, Pt(4f) spectra were restored to those of the as-prepared Pt/CeO_2 sample. A similar observation is reported by Daniel.[40] The binding energies, relative intensities, and fwhm of different platinum species as observed from Pt(4f) spectra of (a) Pt metal particles, (b) as-prepared 1% Pt/CeO_2, (c) 1% Pt/CeO_2 after CO + O_2 reaction, and (d) as-prepared 2% Pt/CeO_2 are summarized in Table 1.

The surface concentration ratio of Pt/Ce in Pt/CeO_2 catalyst from XPS is estimated following the relative peak area method

TABLE 1: Binding Energies, Relative Intensities and fwhm of Different Platinum Species as Observed from Pt(4f) Spectra of Pt/CeO_2 Catalysts with Various Pt Concentrations at Different Conditions

catalyst	species	binding energy of $Pt4f_{7/2}$ (eV)	relative intensity (%)	fwhm (eV)
Pt metal particles	Pt^0	71.1	100	2.3
1% Pt/CeO_2	Pt^0	71.0	7	2.6
	Pt^{2+}	71.9	72	3.1
	Pt^{4+}	74.3	21	3.3
1% Pt/CeO_2	Pt^0	71.1	6	2.5
(after reaction)	Pt^{2+}	72.4	73	2.9
	Pt^{4+}	74.4	21	3.1
2% Pt/CeO_2	Pt^0	71.0	12	2.4
	Pt^{2+}	72.1	69	2.6
	Pt^{4+}	74.4	21	3.3

suggested by Tougaard.[41] The surface concentration ratio of Pt/Ce is given by

$$\frac{X_{Pt}}{X_{Ce}} = \frac{\lambda_{Pt}(E_{Pt})a^3(CeO_2)\lambda_{Pt/CeO_2}(E_{Ce})I_{Pt}(Pt/CeO_2)/I_{Pt}(Pt)}{\lambda_{Ce}(E_{Ce})a^3(Pt)\lambda_{Pt/CeO_2}(E_{Pt})I_{Ce}(Pt/CeO_2)/I_{Ce}(CeO_2)} \quad (1)$$

where X, λ, a, and I are the surface concentration, inelastic mean free path, lattice parameter, and peak intensity, respectively. XPS core level spectra of Pt(4f) and Ce(3d) were recorded for Pt metal particles, Pt/CeO_2, and pure CeO_2 under identical experimental conditions. Inelastic mean free path values have been obtained from the literature.[42] Lattice parameters of CeO_2 and Pt are 5.4112 and 3.923 Å, respectively. Integrated intensities of Pt(4f) core level peaks in Pt nanoparticles and Pt/CeO_2 and Ce(3d) core level peaks in pure CeO_2 and Pt/CeO_2 have been taken into account to calculate the concentration. Accordingly, the Pt/Ce concentration ratio in 1% Pt/CeO_2 is found to be 0.095. Thus, surface concentration of Pt in 1% Pt/CeO_2 is 9.5%. Similarly, that of Pt in 2% Pt/CeO_2 is 15%. We also find that there is no decrease in surface concentration of Pt in 1% Pt/CeO_2 sample after CO + O_2 reaction for 25 h.

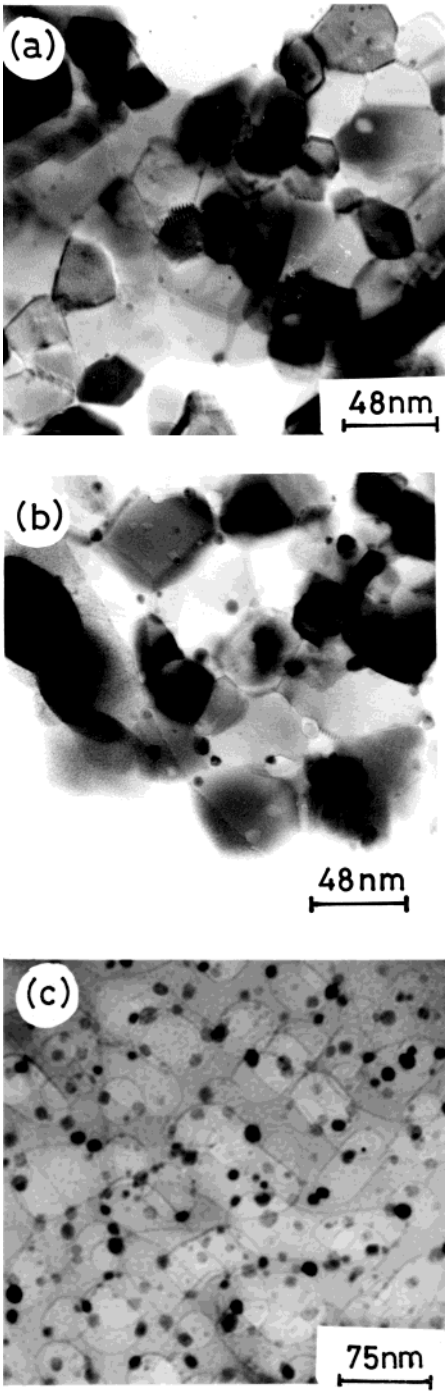

Figure 7. TEM of as-prepared (a) 1% Pt/CeO_2, (b) 2% Pt/CeO_2, and (c) 1% Pt/Al_2O_3.

FTIR Studies. Figure 12 shows FTIR of CO over as-prepared Pt metal particles and 1% Pt/CeO_2 at different conditions. The IR spectrum of CO on as-prepared Pt metal contains three peaks at 2176, 2111, and 2082 cm^{-1} when 5% CO in He was flowing over the sample (Figure 12a). When CO flow was stopped and purged with pure He, only the peak at 2082 cm^{-1} is seen. The lower frequency peak at 2082 cm^{-1} should then correspond to more strongly chemisorbed CO over Pt. Considering that this peak could be due to oxidized Pt, the sample was reduced by heating in a CO + He flow at 200 °C for 15 min in the IR cell and cooled to room temperature in a CO + He flow. Peaks at 2176 and 2111 cm^{-1} remain unaltered, whereas the peak at 2082 cm^{-1} disappeared. However, 2176 and 2111 cm^{-1} peaks also disappeared when the CO + He flow was stopped and purged with He. Therefore, the peak at 2082 cm^{-1} is associated with the oxidized Pt.

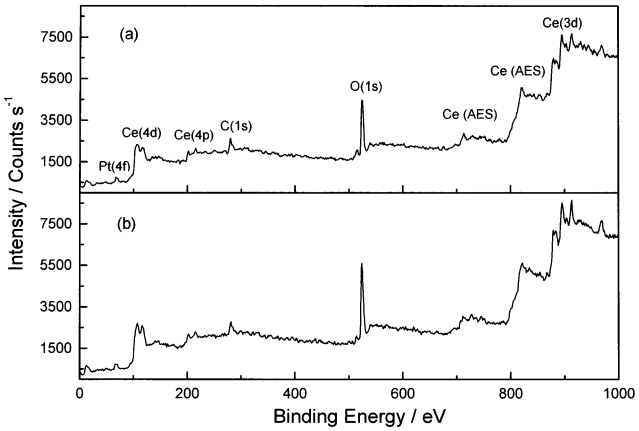

Figure 8. XPS survey spectra taken from 1% Pt/CeO_2 (a) before and (b) after CO + O_2 reaction.

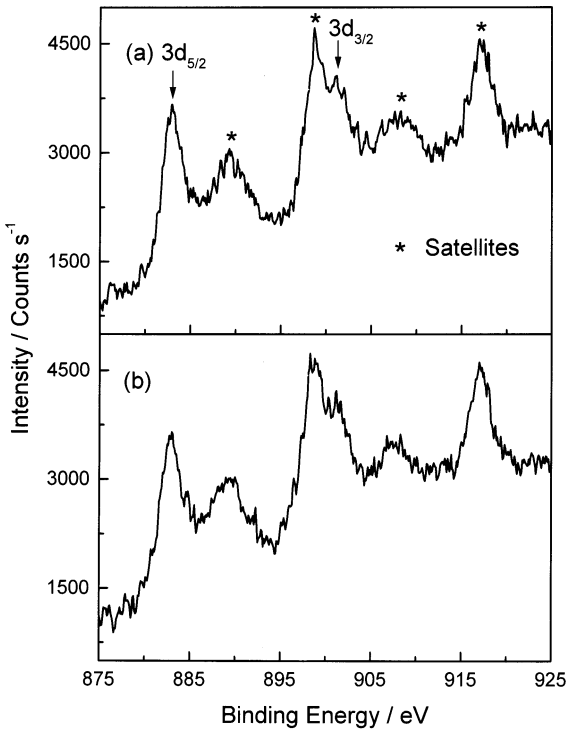

Figure 9. XPS of core level region of Ce(3d) in 1% Pt/CeO_2 (a) before and (b) after CO + O_2 reaction.

Under the CO flowing condition over as-prepared 1% Pt/CeO_2, three peaks are observed at 2176, 2111, and 2082 cm^{-1}. When the CO + He flow was stopped and purged with He, the strong peak at 2082 cm^{-1} remains unchanged with a broad lower frequency tail (Figure 12c), and a small peak at 2164 cm^{-1} is also observed in the higher frequency region. Therefore, the peak at 2082 cm^{-1} over Pt/CeO_2 coincident with that of 2082 cm^{-1} over oxidized Pt metal indeed supports the presence of oxidized Pt in Pt/CeO_2.

There are several IR studies of CO on Pt, Pt/Al_2O_3, $Pt/CeO_2/Al_2O_3$, and Pt/CeO_2 catalysts. Two peaks at 2090 and 2081 cm^{-1} are observed when CO + O_2 was passed over $Pt/CeO_2/Al_2O_3$ samples heated at different temperatures.[16] Coadsorption of CO and O_2 over Pt shows a peak at 2061 cm^{-1} which coincides with CO_2 adsorption over Pt/CeO_2.[18] The strong peak at 2061 cm^{-1} is largely attributed to adsorption of CO over Pt site that is already bonded to oxygen. The low CO stretching frequency

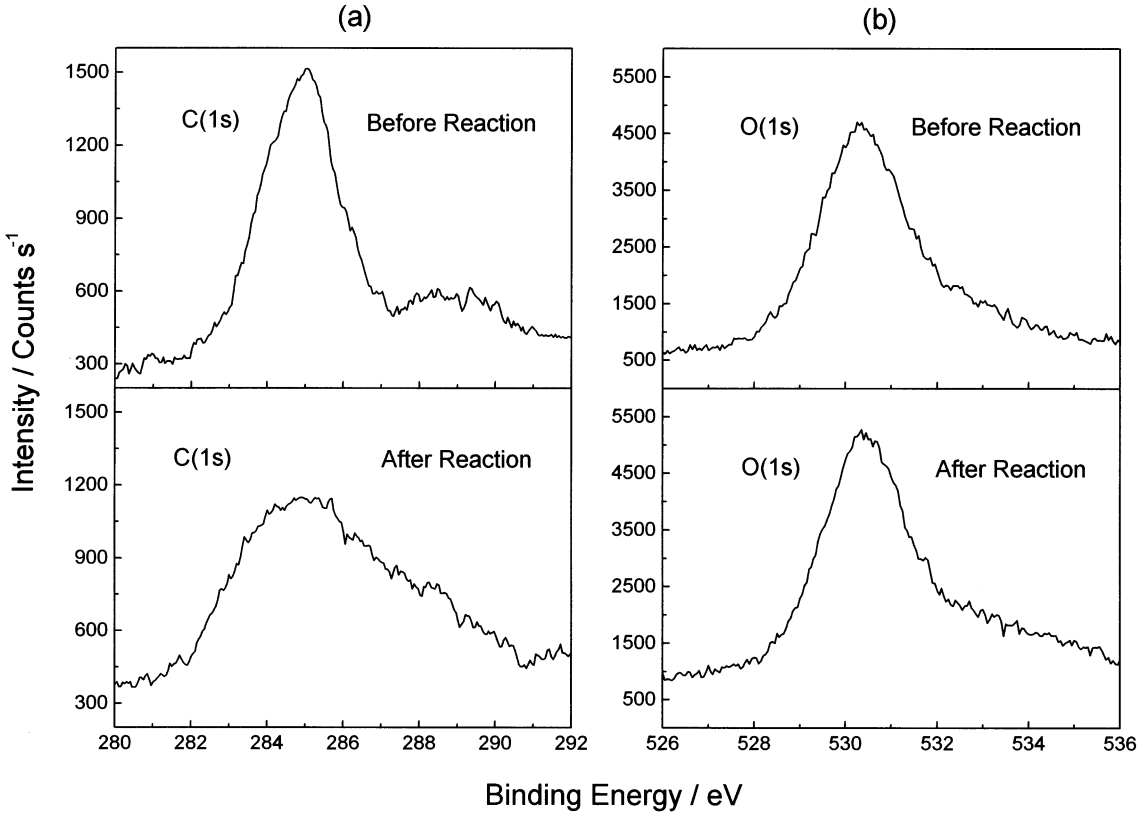

Figure 10. XPS of core level regions of (a) C(1s) and (b) O(1s) before and after CO + O_2 reaction in 1% Pt/CeO_2.

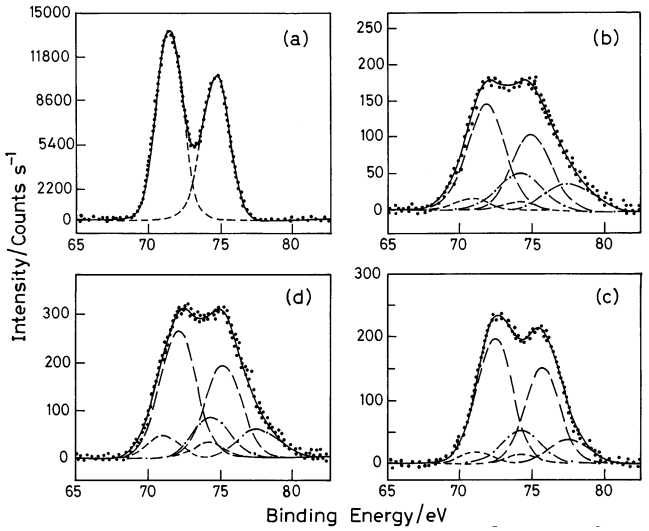

Figure 11. XPS of core level region of Pt(4f) in (a) Pt metal particles, (b) as-prepared 1% Pt/CeO_2, (c) 1% Pt/CeO_2 after CO + O_2 reaction, and (d) as-prepared 2% Pt/CeO_2.

at 2061 cm^{-1} may be due to the precursor to CO_2 formation. The strong CO adsorption peak over 2% Pt/CeO_2 at 2085 cm^{-1} obtained by Jin et al.[18] indeed agrees well with our present study. IR studies of CO and CO_2 adsorption on Pt/CeO_2 by Daniel also show CO stretching frequency around 2080 cm^{-1}.[40] He has suggested the oxidation of Pt by the CeO_2 support and an enhanced stability of CO on oxidized Pt. All these studies clearly indicate that CO is chemisorbed strongly with a stretching frequency around 2082 cm^{-1} on oxidized Pt.

Discussion

The promoting effect of CeO_2 in Pt/CeO_2 catalyst for CO oxidation can be seen quantitatively in Figure 1. For example, at 200 °C, the CO conversion rate over 1% Pt/CeO_2 is 1.13 × 10^{-3} mol g^{-1} (Pt) s^{-1}, whereas it is 1.32 × 10^{-5} mol g^{-1} (Pt) s^{-1} over Pt metal particles. Thus, the rate is 85 times higher on 1% Pt/CeO_2 than on pure Pt metal particles. Further, activation energy is much lower for 1% Pt/CeO_2 in comparison with Pt metal particles. In the case of Pt metal particles (6−7 nm in size), only the surface atoms contribute to the active sites. Assuming Pt metal particle surface as consisting of (100) planes having 1.3 × 10^{15} Pt atoms cm^{-2}, the ratio of the total number of Pt atoms in 6.5 nm spherical Pt particles to the number of surface Pt atoms of the same particle is found to be 4.77. This indicates that even if all the atoms in the Pt metal particle are dispersed over the CeO_2 surface as Pt atoms, the increase in the actual rate of CO oxidation over 1% Pt/CeO_2 should have been about 5 times more than Pt particles. But, the increase in CO oxidation rate over 1% Pt/CeO_2 is observed to be much higher than a factor of 5, which seems to come from Pt−CeO_2 interaction. Therefore, it is essential to understand the structure of the Pt/CeO_2 catalyst.

The combustion method involves rapid heating of an aqueous solution containing stoichiometric amounts of corresponding metal nitrates and hydrazine-based fuels. Evolution of large amounts of gases during the process is responsible for fine crystallite formation. During the combustion, the reaction temperature reaches above 1000 °C for a short period (30−60 s) and then is cooled to ∼300 °C in less than a minute. Thus, the oxide formed at high temperature is quenched in this process. So in the combustion-derived 1% Pt/CeO_2, Pt ions should either get separated into Pt metal particles as in 1% Pt/Al_2O_3[28] or platinum oxide particles separated from oxide support or platinum ions should get incorporated into the CeO_2 matrix.

In the XRD pattern about 0.08% Pt metal out of 1 at. % Pt is indeed detected. If any of the oxides of Pt are formed, even at the 0.08% level, it could have been detected in the XRD. In the TEM also, about 0.05% Pt is seen as metal particles out of

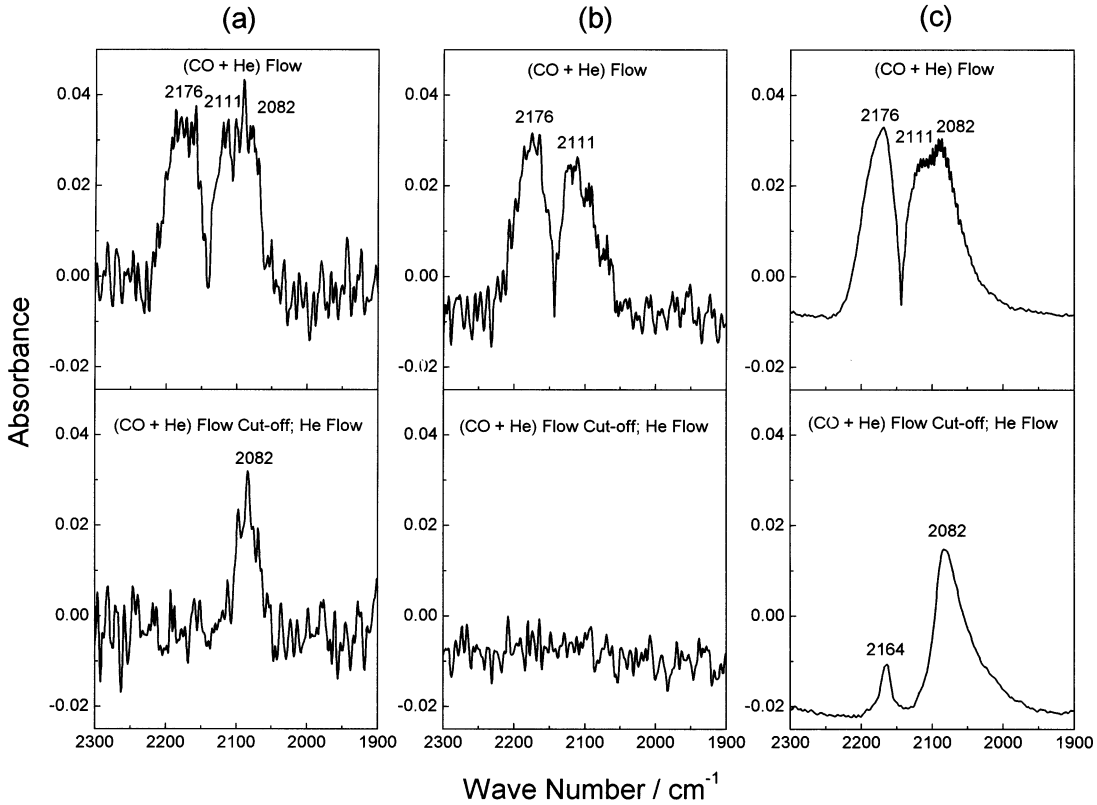

Figure 12. FTIR spectra of CO on (a) Pt metal particles, (b) reduced Pt metal particles, and (c) 1% Pt/CeO_2 at different conditions at room temperature.

1% Pt taken in the preparation. In XPS studies, it is shown that about 0.07% Pt in 1% Pt/CeO_2 are in metallic state. Even though, at 1 at. % Pt level, it is difficult to ascertain Pt ion substitution; high resolution XRD studies presented here certainly indicate the substitution of Pt^{2+} in the Ce^{4+} site by way of decrease in lattice parameter and total lattice oxygen compared to pure CeO_2. This is further substantiated by the fact that a PtO or PtO_2 phase could not be detected from any of the experimental techniques studied here. Even though a small amount of Pt (0.08% in 1% Pt/CeO_2) particles are detected, Pt metal particles cannot be the active sites for CO adsorption in 1% Pt/CeO_2 because the temperature at which the CO to CO_2 reaction over Pt metal particles occurs is much higher than that over 1% Pt/CeO_2 (see Figure 1). In IR studies, if CO adsorption over Pt/CeO_2 is due to Pt metal particles only, then the peak at 2082 cm^{-1} should have disappeared on stopping the CO + He flow over 1% Pt/CeO_2. The major difference between Pt/CeO_2 and Pt metal particle catalyst is the presence of Pt, mostly in the Pt^{2+} state in Pt/CeO_2.

XRD, TEM, and XPS studies show that the Pt ions seem to get incorporated into the CeO_2 matrix due to low metal loading (1% by mole) and the highly ionic nature of CeO_2 compared to Al_2O_3. A solid solution of the type $Ce_{1-x}Pt_xO_{2-\delta}$ is one of the routes of incorporation of ions in CeO_2. Ionic radii of Pt^{2+} (80 pm) is closer to that of Ce^{4+} (97 pm).[43] Therefore, if these metal ions are formed in the preparation condition, Pt^{2+} ions can form solid solution of the type $Ce_{1-x}Pt_xO_{2-\delta}$. If there is an ionic substitution of Pt^{2+} ions for Ce^{4+} sites in CeO_2, the lattice parameter should decrease and an oxide ion vacancy should be created in order to maintain the charge neutrality due to lower valent ionic substitution. Rietveld analysis of XRD data did show the presence of oxide ion vacancy and a decrease in the CeO_2 lattice parameter. Although absolute oxide ion vacancy is difficult to ascertain due to a large variation in scattering cross section of cerium and oxygen, an increase of oxide ion vacancy from 3.5 to 5% in pure CeO_2 to 1% Pt/CeO_2 certainly indicates the presence of oxide ion vacancies. Further, over 70% Pt in the +2 state as seen from XPS supports the occurrence of oxide ion vacancy if Pt^{2+} ions are incorporated into the CeO_2 lattice for the charge balancing requirement. Observation of nearly 10 times more surface concentration of Pt^{2+} compared to 1 at. % Pt taken in the preparation suggests that Pt^{2+} ions are on the surface. Since there is a decrease in the lattice parameter, the oxide ion vacancy seems to be concentrated on the surface associated with lower valent Pt^{2+} ions. Indeed, we have recently shown that Pd^{2+} and Cu^{2+} ions are mostly on the surface and oxide ion vacancies are around the Pd^{2+} and Cu^{2+} ions in $Ce_{1-x}Pd_xO_{2-\delta}$ and $Ce_{1-x}Cu_xO_{2-\delta}$, respectively.[44,45] From the above studies, we suggest that the Pt/CeO_2 catalyst consists of ~30 nm $Ce_{1-x}Pt_xO_{2-\delta}$ crystallites where Pt in mostly the +2 state occupying the Ce^{4+} site creates oxide ion vacancy. Such a structure provides $-Ce^{4+}-O^{2-}-Pt^{2+}-\square-$ linkages. Total Pt content being low (just 1 at. %), even if all of the Pt taken are dispersed over the surface of ~30 nm CeO_2 crystallites, not more than 15−20% of Ce^{4+} ion on the surface can be replaced by Pt ions.[46] Therefore, Pt^{2+} ions seem to be present as isolated ions substituted for the Ce^{4+} site on Pt/CeO_2 crystallite surface. However, small patches of a PtO layer over CeO_2 cannot be ruled out.

To obtain higher rates of CO conversion, it is not sufficient alone that a larger number of CO adsorption sites is created. A corresponding increase in the availability of dissociated oxygen is essential. Even though lattice oxygen is utilized for CO_2 formation, as seen from Figure 2, yield is low for the same CO flow compared to when feed oxygen is present. Therefore, additional sites for O_2 adsorption/dissociation are needed. Partial pressure of oxygen in the gas is higher than that in the catalyst and, hence, oxygen occupancy in the vacant oxide ion site is a distinct possibility. Therefore, we suggest that oxide ion vacancy in CeO_2 created by Pt^{2+} ion substitution can become an oxygen

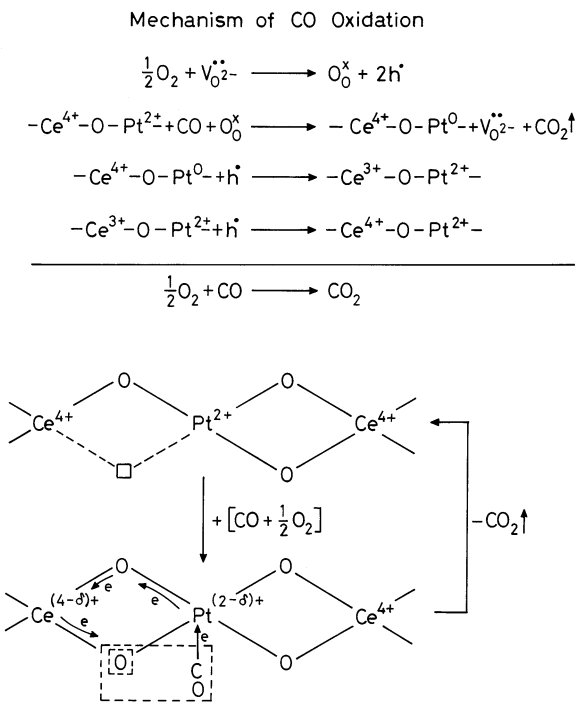

Figure 13. Schematic representation of CO + O_2 reaction over 1% Pt/CeO_2 where $V_{O^{2-}}^{\bullet\bullet}$, O_O^x, and $h^\bullet$ are doubly ionized oxide ion vacancy, neutral oxygen occupied in the vacancy, and electron hole, respectively.

adsorption/dissociation site. Based on the $Ce_{1-x}Pt_xO_{2-\delta}$ model, the CO oxidation mechanism is depicted in Figure 13, where, $V_{O^{2-}}^{\bullet\bullet}$, O_O^x, and $h^\bullet$ are doubly ionized oxide ion vacancy, neutral oxygen occupied in the vacancy, and electron hole, respectively. It is important to note that in addition to the Pt^{2+}/Pt^0 redox couple, the Ce^{4+}/Ce^{3+} couple is involved in this model. Delocalization of electrons from Pt^0 can easily occur to Ce(4f) levels due to the proximity of Pt^{2+} and Ce^{4+} provided by the $-Ce^{4+}-O^{2-}-Pt^{2+}-\square-$ linkages in the lattice. This model supports the experimental observation of the promoting effect of CeO_2 such as high oxygen storage capacity at low temperature, higher dispersion of Pt, and prevention of sintering due to separation of Pt in the form of Pt^{2+} ions.

Conclusions

The main features of this investigation are: (1) single-step preparation of 1% Pt/CeO_2 nanocrystallites by the solution combustion technique; (2) platinum is stabilized mainly in +2 oxidation state on nanosized CeO_2 in the form of $Ce_{1-x}Pt_xO_{2-\delta}$ like phase; (3) platinum ions are the active sites in Pt/CeO_2 catalyst for CO oxidation. (4) Pt^{2+}/Pt^0 coupled with Ce^{4+}/Ce^{3+} via oxygen vacancy is suggested to facilitate low-temperature redox reactions; (5) the promoting action of CeO_2 in Pt/CeO_2 catalyst is due to the ionic dispersion of platinum leading to $-Ce^{4+}-O^{2-}-Pt^{2+}-\square-$ linkages.

Acknowledgment. A.G. thanks the Council of Scientific and Industrial Research (CSIR), Government of India, for the award of a research fellowship. Thanks are due to N. Sivasankar and Professor S. Vasudevan of the Department of Inorganic and Physical Chemistry, Indian Institute of Science for providing the FTIR facility. Financial support from the Department of Science and Technology (DST), Government of India, is gratefully acknowledged.

Note Added after ASAP Posting. This article was posted ASAP on the Web on 5/28/2003. Changes were made to the caption for Figure 11d. The correct version was posted on 5/30/2003.

References and Notes

(1) Augustine, R. L. *Heterogeneous Catalysis for the Synthetic Chemist*; Marcel Dekker: New York, 1996; p 153.
(2) Taylor, K. C. *Catal. Rev. −Sci. Eng.* **1993**, *35*, 457.
(3) Yu Yao, Y.-F. *Ind. Eng. Chem. Prod. Res. Dev.* **1980**, *19*, 293.
(4) Bauerle, G. L.; Wu, S. C.; Nobe, K. *Ind. Eng. Chem. Prod. Res. Dev.* **1975**, *14*, 123.
(5) Kobylinski, T. P.; Taylor, B. W. *J. Catal.* **1974**, *33*, 376.
(6) Takoudls, C. G.; Schmidt, L. D. *J. Phys. Chem.* **1983**, *87*, 964.
(7) Yao, H. C.; Yu Yao, Y.-F. *J. Catal.* **1984**, *86*, 254.
(8) Kummer, J. T. *J. Phys. Chem.* **1986**, *90*, 4747.
(9) Burch, R. *Pure Appl. Chem.* **1996**, *68*, 377.
(10) Seker, E.; Gulari, E. *J. Catal.* **2000**, *196*, 4.
(11) Kim, G. *Ind. Eng. Chem. Prod. Res. Dev.* **1982**, *21*, 267.
(12) Summers, J. C.; Ausen, S. A. *J. Catal.* **1979**, *58*, 131.
(13) Lööf, P.; Kasemo, B.; Andersson, S.; Frestad, A. *J. Catal.* **1991**, *130*, 181.
(14) Oh, S. H.; Mitchell, P. J.; Siewert, R. M. *J. Catal.* **1991**, *132*, 287.
(15) Nunan, J. G.; Robota, H. J.; Cohn, M. J.; Bradley, S. A. *J. Catal.* **1992**, *133*, 309.
(16) Martínez-Arias, A.; Coronado, J. M.; Cataluña, R.; Conesa, J. C.; Soria, J. *J. Phys. Chem. B* **1998**, *102*, 4357.
(17) Jin, T.; Okuhara, T.; Mains, G. J.; White, J. M. *J. Phys. Chem.* **1987**, *91*, 3310.
(18) Jin, T.; Zhou, Y.; Mains, G. J.; White, J. M. *J. Phys. Chem.* **1987**, *91*, 5931.
(19) Cox, D. F.; Hoflund, G. B.; Laitinen, H. A., *Langmuir* **1985**, *1*, 269.
(20) Schryer, D. R.; Upchurch, B. T.; Sidney, B. D.; Brown, K. G.; Hoflund, G. B.; Herz, R. K. *J. Catal.* **1991**, *130*, 314.
(21) Gardner, S. D.; Hoflund, G. B.; Upchurch, B. T.; Schryer, D. R.; Kielin, E. J.; Scheyer, J. *J. Catal.* **1991**, *129*, 114.
(22) Gardner, S. D.; Hoflund, G. B.; Schryer, D. R.; Scheyer, J.; Upchurch, B. T.; Kielin, E. J. *Langmuir* **1991**, *7*, 2135.
(23) Gardner, S. D.; Hoflund, G. B.; Davidson, M. R.; Laitinen, H. A.; Schryer, D. R.; Upchurch, B. T. *Langmuir* **1991**, *7*, 2140.
(24) Haruta, M.; Yamada, N.; Kobayashi, T.; Iijima, S. *J. Catal.* **1989**, *115*, 301.
(25) Haruta, M.; Tsubota, S.; Kobayashi, T.; Kageyama, H.; Genet, M. J.; Delmon, B. *J. Catal.* **1993**, *144*, 175.
(26) Epling, W. S.; Hoflund, G. B.; Weaver, J. F.; Tsubota, S.; Haruta, M. *J. Phys. Chem.* **1996**, *100*, 9929.
(27) Bera, P.; Aruna, S. T.; Patil, K. C.; Hegde, M. S. *J. Catal.* **1999**, *186*, 36.
(28) Bera, P.; Patil, K. C.; Jayaram, V.; Hegde, M. S.; Subbanna, G. N. *J. Mater. Chem.* **1999**, *9*, 1801.
(29) Bera, P.; Patil, K. C.; Hegde, M. S. *Phys. Chem. Chem. Phys.* **2000**, *2*, 373.
(30) Pino, L.; Recupero, V.; Beninati, S.; Shukla, A. K.; Hegde, M. S.; Bera, P. *Appl. Catal. A* **2002**, *2*, 63.
(31) Perrichon, V.; Laachir, A.; Bergeret, G.; Fréty, R.; Tournayan, L.; Touret, O. *J. Chem. Soc., Faraday Trans.* **1994**, *90*, 773.
(32) Terribile, D.; Trovarelli, A.; de Leitenburg, C.; Dolcetti, G.; Llorca, J. *Chem. Mater.* **1997**, *9*, 2676.
(33) Sermon, P. A.; Bond, G. C. *Catal. Rev.* **1973**, *8*, 211.
(34) Conner, W. C., Jr.; Falconer, J. L. *Chem. Rev.* **1995**, *95*, 759.
(35) Hickey, N.; Foransiero, P.; Kašpar, J.; Gatica, J. M.; Bernal, S. *J. Catal.* **2001**, *200*, 181.
(36) Bera, P.; Hegde, M. S.; Patil, K. C. *Curr. Sci.* **2001**, *80*, 1576.
(37) Hariprakash, B.; Bera, P.; Martha, S. K.; Gaffoor, S. A.; Hegde, M. S.; Shukla, A. K. *Electrochem. Solid-State Lett.* **2001**, *4*, A23.
(38) Sarma, D. D.; Hegde, M. S.; Rao, C. N. R. *J. Chem. Soc., Faraday Trans. 2* **1981**, *77*, 1509.
(39) Shyu, J. Z.; Otto, K. *J. Catal.* **1989**, *115*, 16.
(40) Daniel, D. W. *J. Phys. Chem.* **1988**, *92*, 3891.
(41) Tougaard, S. *J. Vac. Sci. Technol. A* **1996**, *14*, 1415.
(42) Penn, D. R. *J. Electron Spectrosc. Relat. Phenom.* **1976**, *9*, 29.
(43) Shannon, R. D. *Acta Crystallogr. A* **1976**, *32*, 751.
(44) Priolkar, K. R.; Bera, P.; Sarode, P. R.; Hegde, M. S.; Emura, S.; Kumashiro R.; Lalla, N. P. *Chem. Mater.* **2002**, *14*, 2120.
(45) Bera, P.; Priolkar, K. R.; Sarode, P. R.; Hegde, M. S.; Emura, S.; Kumashiro, R.; Lalla, N. P. *Chem. Mater.* **2002**, *14*, 3591.
(46) Bera, P.; Patil, K. C.; Jayaram, V.; Subbanna, G. N.; Hegde, M. S. *J. Catal.* **2000**, *196*, 293.